agronomy

MDPI

Article

Microbiology Combined with the Root Metabolome Reveals the Responses of Root Microorganisms to Maize Cultivars under Different Forms of Nitrogen Supply

Guan Tian, Wei Ren, Junping Xu, Xiaoyang Liu, Jiaxing Liang, Guohua Mi, Xiaoping Gong * and Fanjun Chen *

State Key Laboratory of Nutrient Use and Management, College of Resources and Environmental Sciences, China Agricultural University, Beijing 100193, China; tianguancau@126.com (G.T.); renwei2012@126.com (W.R.); xujunping1994@163.com (J.X.); mrliuxiaoyang1@163.com (X.L.); zyjxliang@163.com (J.L.); miguohua@cau.edu.cn (G.M.)

* Correspondence: gongxp@cau.edu.cn (X.G.); caucfj@cau.edu.cn (F.C.); Tel.: +86-010-62734454 (X.G.); +86-010-62734454 (F.C.)

Abstract: Plant–microbe interactions are key to nutrient-use efficiency. Root microbes are influenced by rhizosphere soil and plant cultivars. The impact of cultivar-by-nitrogen (N) interactions on the maize-root microbiome remains unclear, yet it is crucial for understanding N use efficiency in maize. This study evaluated the effects of maize cultivars and N forms, along with their interactions, on the diversity and composition of root bacteria and fungi. Additionally, we examined correlations between soil microbes and root metabolites. The maize cultivar Zhengdan 958 (ZD958) showed a positive response to the mixture of nitrate and ammonium N, resulting in increased in biomass, grain yield, shoot N content, grain N content, and root area. In contrast, the cultivar Denghai605 (DH605) did not exhibit a similar response. The diversity and composition of root bacteria and fungi differed between ZD958 and DH605. The N form primarily affected the community structure of rhizospheric fungi in ZD958 and rhizospheric bacteria in DH605, rather than endophytic microbes. A mixed N supply increased the relative abundance of Basidiomycota, which was positively correlated with ZD958 yield. For DH605, a mixed N treatment enhanced nitrification functions involving Bacteroidetes and Proteobacteria, while it reduced the effects of ammonium N supply. The dominant rhizospheric microbes in DH605 showed a stronger response to changes in root metabolites compared to those in ZD958. A mixed N supply increased the content of palmitoleic acid in ZD958 root exudates, facilitating the recruitment of beneficial rhizospheric microbes, which promotes maize growth. In DH605, a mixed N supply decreased the concentration of sphinganine, which is significantly correlated with Acidobacteria (negatively), Proteobacteria (negatively), Bacteroidetes (positively), and TM7 (positively). Our findings suggest that different maize cultivars respond differently to N forms, causing distinct rhizospheric microbial effects, and that root metabolites send metabolic signals to regulate and recruit key bacterial and fungal communities.

Keywords: maize; microbial; NO_3^--N; NH_4^+-N; root metabolites

Citation: Tian, G.; Ren, W.; Xu, J.; Liu, X.; Liang, J.; Mi, G.; Gong, X.; Chen, F. Microbiology Combined with the Root Metabolome Reveals the Responses of Root Microorganisms to Maize Cultivars under Different Forms of Nitrogen Supply. *Agronomy* **2024**, *14*, 1828. https://doi.org/10.3390/agronomy14081828

Academic Editor: Robert P. Larkin

Received: 8 July 2024
Revised: 30 July 2024
Accepted: 13 August 2024
Published: 19 August 2024

1. Introduction

Microorganisms influencing their host plants include those colonizing the plant surface and those entering plant tissues; they are collectively known as the plant microbiome [1]. Together with the plant genome, they regulate plant growth and development [2]. Recent research has extensively explored the plant microbiome's role in nutrient uptake, crop antagonism, and resistance to pests and diseases [3]. Thus, understanding how microbial communities interact with their environment and influence plant growth in specific conditions is crucial.

Nitrogen (N) is vital for plant growth and development. Globally, maize (*Zea mays* L.)-grain yield improvements largely depend on N fertilizer input [4]. Despite the substantial

application of N fertilizers in agriculture, approximately 50% of the applied nitrogen is effectively absorbed by crops due to its inefficient utilization [5]. Nitrate (NO_3^--N) and ammonium (NH_4^+-N) are the primary inorganic N forms available to plants [6]. NO_3^--N predominate in well-aerated soils, while NH_4^+-N is present at much lower concentrations [7]. NH_4^+-N metabolism typically consumes less energy than NO_3^--N assimilation [8], and different crop species exhibit preferences for NO_3^--N or NH_4^+-N based on evolutionary adaptations [9]. Genotypic variations among crops in different soil conditions significantly influence N-form preferences, affecting yield and N uptake characteristics [10,11]. For maize, a mixed N supply has been shown to promote growth effectively [12,13]. However, $NH4^+$-N in soil converts quickly to NO_3^--N due to nitrifying bacteria converting ammonium to nitrate and denitrifying bacteria converting ammonium to nitrogen gas. Unlike nitrate nitrogen, which can persist in the soil for extended periods, this rapid conversion highlights the need to adjust ammonium-nitrate ratios to optimize maize yield [13]. The nitrogen cycle is a cornerstone of the soil ecosystem, driven by microorganisms through processes like N-fixation, ammonification, nitrification, and denitrification [14]. Nitrification, linking N-fixation and denitrification, occurs in two stages: NH_4^+ conversion to NO_2^- and then to NO_3^- [15]. Ammonia oxidation involves bacteria primarily found in Proteobacteria subgroups B and C, containing amoA, amoB, and amoC genes encoding ammonia monooxygenase [16]. Nitrite oxidation is carried out by various bacteria, including Nitrospinae (Deltaproteobacteria), Nitrospirae, Nitrobacter (Alphaproteobacteria), and Nitrococcus (Gammaproteobacteria). Nitrification significantly impacted plant N use efficiency (NUE) [17], emphasizing the need to apply N fertilizers tailored to plant N preferences.

Nitrogen application profoundly alters microbial community structure and diversity [6,18,19], both in external plant tissues and within plant roots [20,21]. Previous studies indicate that N fertilization reduces microbial biomass carbon and bacterial diversity [22] and directly inhibits ammonium-oxidizing bacteria and archaea due to high ammonium levels [23–25]. Additionally, N fertilization shifts microbial communities from Alphaproteobacteria to Gammaproteobacteria, influencing denitrification, nitrification, and N fixation [26]. Moreover, N fertilization increases Proteobacteria and Actinobacteria abundance while decreasing Acidobacteria [27]. Yet, the specific effects of different N forms (NH_4^+-N vs. NO_3^--N) on rhizospheric microbial communities and associated N transformations remain poorly understood.

Root metabolites released into the rhizosphere play crucial roles in nutrient cycling, energy flow, and organic matter turnover [28]. The composition of root metabolites is significantly influenced by the amount and form of N [13,29,30]. Approximately 20% of photosynthetically assimilated carbon is exuded into the rhizosphere, altering metabolite quantities [7]. Consequently, root metabolite changes likely reshaped rhizospheric microbial communities, impacting plant growth and N utilization efficiency [17]. However, it remains unclear whether maize exposed to different N forms recruits specific microbes to modulate growth through altered root metabolites.

This study focused on maize cultivars exhibiting differential responses to various N forms, exploring how cultivars-by-nitrogen interactions reshaped root bacterial and fungal communities. Our objectives are to (i) investigate the effects of N forms and cultivars on plant growth, rhizospheric and endophytic microbes, and root metabolites, and (ii) explore correlations between specific microbial taxa and root metabolites, potentially elucidating how maize recruits microbes to process different N forms effectively.

2. Materials and Methods

2.1. Plant Materials and Growth Conditions

Field experiments were conducted at the ShangZhuang Experimental Station of China Agricultural University in Beijing (latitude 40°38′ N, longitude 116°0′ E) in 2018 and 2019. Four maize cultivars—Zhengdan958 (ZD958), Weike702 (WK702), Denghai605 (DH605), and Longping206 (LP206)—widely grown commercial hybrids in China were evaluated

with two forms of nitrogen: nitrate only and a mix of ammonium and nitrate. Microorganisms and root metabolites were sampled and analyzed only in 2019.

The field trials were designed using a split-plot layout with four replications each year. The main plots contained one of two nitrogen forms: nitrate nitrogen (NO_3^--N) and a mix of ammonium and nitrate nitrogen (NH_4^+-N + NO_3^--N). The plots were fertilized with 135 kg ha^{-1} P_2O_5 and 100 kg ha^{-1} K_2O 10 days before sowing. A total of 180 kg ha^{-1} N was applied using two N forms: calcium nitrate (NO_3^--N) and a mix of ammonium sulfate and calcium nitrate (NO_3^--N:NH_4^+-N = 1:1). The N fertilizers were applied in four stages: 20% (36 kg ha^{-1} N) at the third leaf stage (V3, 25 days after sowing), 30% (54 kg ha^{-1} N) at the sixth leaf stage (V6, 35 days after sowing), 20% (36 kg ha^{-1} N) at the tenth leaf stage (V10, 50 days after sowing), and 30% (54 kg ha^{-1} N) at the silking stage (R1, 65 days after sowing). Soil physical and chemical characteristics were evaluated at the beginning of the experiment. The topsoil layer (0–30 cm) contained organic matter at 15.1 g kg^{-1}, NaOH-N at 21.5 mg kg^{-1}, available phosphorus (Olsen-P) at 16.1 mg kg^{-1}, ammonium acetate extractable potassium (NH4Ac-K) at 133 mg kg^{-1} and pH 7.22 (1:1.25 g/v) [31]. Subplots in each main plot contained each of the four cultivars. Each subplot was 4 m long, with seven rows of each cultivar. Row and plant spacing were 0.5 m and 0.33 m, respectively. Each row contained 13 plants. Two seeds of each maize cultivar were sown per hole at a depth of 5 cm using sowing tools. At the V3, seedlings were thinned to achieve a final density of 60,000 plants ha^{-1}.

2.2. Plant Sampling, N Accumulation, and Yield Measurement

Field data were collected from the five middle rows of each plot, with the outer rows serving as borders. At the R1 stage and physiological maturity (R6) stage, five consecutive plants with similar aboveground growth from each replicate were cut at the soil surface and separated into leaves, stalks (including leaf sheaths, tassel, husks, and either cobs at R6 or ear-shoots at R1), and grain. All sampled plants were oven-dried at 105 °C for 30 min and then dried at 70 °C until reaching a constant weight. Dry matter weights were recorded, and the samples were ground into fine powder for N measurements. N concentration was determined using a modified Kjeldahl digestion assay. At physiological maturity, the ears in the middle three rows were harvested to measure fresh weight. One row of ears was randomly selected from the central three rows of each subplot and then threshed. The grain was oven-dried to determine moisture content at harvest, and grain yield was standardized to 14% moisture.

2.3. Microbial Sample Preparation and Root Architecture Measurements

After cutting off the shoots at the silking stage, plant roots (0–20 cm depth) were excavated following Shao et al. [32]. The roots were gently shaken to remove most of the adhering soil. Five roots were dug from each replicate by a shovel, and large soil chunks were removed. Two or three active seminal roots were cut from each root system and stored on dry ice for microbiome and root metabolite analysis. Rhizosphere soil from the root surface was used to determine the rhizospheric microbiome, following Beckers et al., while endospheric microbiome processing was based on Becker's method. Root compartments were cleared from epiphytic bacteria through sequential washing: (a) sterile Millipore water (30 s), (b) 70% (*v*/*v*) ethanol (2 min), (c) sodium hypochlorite solution (2.5% active Cl^- with 0.1% Tween 80) (5 min), and (d) 70% (*v*/*v*) ethanol (30 s). Samples were then rinsed five times with sterile Millipore water. Plant samples were cut into small fragments with a sterile scalpel and macerated in sterile phosphate saline buffer (PBS; 130 mM NaCl, 7 mM Na_2HPO_4, 3 mM NaH_2PO_4, pH 7.4) using a Polytron (eppendorf) PR1200 mixer (Kinematica A6). Sterilization and homogenization were conducted under aseptic conditions in a laminar airflow hood. Quadruplicate aliquots (1.5 mL) of each maize-root sample were stored at −80 °C until DNA extraction. The remaining roots were washed with sterile water and placed on dry ice for root metabolite determination.

The cleaned root systems were transferred to a stable-light-source photo studio to capture two-dimensional images. Root Estimator for Shovelomics Traits (REST, Version 1.0.1) software in MatLab 7.12 was used for the quantitative analysis of the root system architecture, including root area and root angle [32]. Root biomass was measured after drying the roots.

2.4. Bioinformatics Analysis of 16S and ITS rRNA Gene Profiling

Metagenomic DNA was extracted from the root samples (0.5 g each) using a FastDNA SPIN Kit (MP Biochemicals, Solon, OH, USA). The DNA quality was assessed by electrophoresis on a 1% agarose gel and by measuring the absorbance at OD260 and OD280 using spectrophotometry. PCR was performed on the extracted DNA targeting the V3–V4 region of 16S and the ITS1 region of ITS. The PCR conditions were as follows: 95 °C for 30 s; 35 cycles of 95 °C for 30 s, 55 °C for 30 s, and 72 °C for 30 s, with a final extension at 72 °C for 10 min. PCR products were examined by agarose gel electrophoresis and purified using AMPure XP Beads (Beckman Coulter, Inc., Brea, CA, USA) following the manufacturer's protocol. An additional eight-cycle PCR was carried out to add dual-index barcodes and Illumina sequencing adapters to each sample, after which the PCR products were again purified using AMPure beads. Equimolar amounts of PCR products from each sample were mixed and sequenced using the Illumina MiSeq PE300 platform. Raw sequence data were processed using Qiime2. Filtered sequences were aggregated into OTUs with 97% similarity. Representative sequences were filtered using UPARSE. OTUs were compared with the SILVA 132 (16S) and UNITE (ITS) databases, and the OTU table was generated by USEARCH. Diversity analysis was conducted using Qiime2. Microbial metabolism and ecological functions were annotated using FAPROTAX (Functional Annotation of Prokaryotic Taxa) software. By inputting the OTU table under different N forms, we determined the ecological functions related to nitrogen.

2.5. Extraction, Determination, and Analysis of Metabolites

Fresh maize-root tissue was ground in a bowl with the continuous addition of liquid nitrogen to maintain low temperature. The ground tissue was freeze-dried, and 20 mg of the sample was weighed into a 2 mL EP tube. Subsequently, 1 mL of extraction solvent (methanol: acetonitrile: water = 2:2:1) was added, followed by vortexing for 30 s, homogenization at 35 Hz for 4 min, and sonication for 5 min on ice. This cycle of homogenization and sonication was repeated three times. The samples were then incubated at −40 °C for 1 h and centrifuged at 12,000 rpm for 15 min at 4 °C. The supernatant was transferred to a fresh glass vial for analysis. A quality control (QC) sample was prepared by combining equal aliquots of the same sample supernatants. The extract was dried in a vacuum concentrator.

Next, 120 µL of methoxyamine salt reagent (methoxyamine hydrochloride, dissolved in pyridine at 20 mg mL^{-1}) was added to the dried metabolites and mixed gently. Subsequently, 120 µL BSTFA (containing 1% TMCS, v/v) was added to each sample. The mixture was incubated at 70 °C for 1.5 h, cooled to room temperature, and then 5 µL FAMEs (dissolved in chloroform) was added for on-machine detection using GC-MS. GC-MS analysis was performed at Biomarker Technologies (BMK). The raw data were converted to the mzXML format using ProteoWizard and processed with an in-house program developed using R, based on XCMS, for peak detection, extraction, alignment, and integration. For metabolite annotation, we utilized an in-house MS2 database (BiotreeDB), with a cutoff set at 0.3. The relative contents of metabolites were calculated according to corrected mass spectra peak areas. Differentially accumulated metabolites (DAMs) between different comparison groups were identified using the following criteria: $|\log_2(\text{fold-change})| \geq 2$ and $p < 0.05$.

2.6. Statistical Analysis

Using the tidyverse package and ggplot2 package in R (3.6.2), we performed analysis of variance (ANOVA) and least significant difference (LSD) analysis to assess the impact of nitrogen forms on crop biomass, soil microorganisms, root metabolites, and the root system architecture. Utilizing the psych package in R, we conducted Pearson correlation analysis between metabolites and bacterial groups, as well as between bacterial and fungal groups. Additionally, we employed the Bray–Curtis dissimilarity distance matrix for ANOVA analysis to identify significant differences in bacterial and fungal communities among different treatment samples.

3. Results

3.1. Maize Genotypic Differences in Response to N Forms

To investigate the response of maize to NO_3^--N and (NH_4^++NO_3^-)-N, four maize cultivars were used over two years. Three-way ANOVAs indicated that grain shoot biomass and grain yield were significantly affected by year, N form, cultivar, year × cultivar interaction, and N form × cultivar interaction (Table S1). Furthermore, the N form, cultivar, year × cultivar interaction, and N form × cultivar interaction significantly affected shoot and grain N contents. The year did not significantly affect shoot and grain N contents, suggesting stability over the two years (Table S1). There were no interactive effects between the two years and N form for biomass, yield, and N content, indicating that these measures are less susceptible to environmental changes (Table S1).

Growth responses to the different N forms were then assessed for each maize cultivar individually. Compared with NO_3^--N treatment, the ammonium and nitrate mixed treatment significantly increased the yields of ZD958 and WK702 in both years. Specifically, the yield of ZD958 increased by 8.8% and 12.8%, while WK702 increased by 7.2% and 10.8% in 2018 and 2019, respectively (Figure 1A,B). The yields of DH605 in 2018 and LP206 in 2019 did not differ between the two N forms (Figure 1A,B). However, compared to the nitrate treatment, the yield of DH605 decreased by 9.4% in 2019, and LP206 decreased by 7.9% in 2018 under mixed N treatment (Figure 1A,B). The shoot biomass of ZD958 increased by 12.8% and 12.1% in 2018 and 2019, respectively, with mixed N treatment; the shoot biomasses of WK702 increased by 16.9% and 13.8%, respectively (Figure 1C,D). For ZD958 and WK702, the mixed N treatment resulted in higher shoot and grain N contents than when only nitrate was supplied in both years (Figure 1E,H). In contrast, DH605 exhibited lower shoot and grain N contents under the mixed N treatment compared to nitrate treatment (Figure 1E,H). For LP206, no differences were found in shoot and grain N contents in response to nitrate or mixed N sources in both years (Figure 1E,H). These results suggest that ZD958 and WK702 have distinct growth responses to NO_3^--N and mixed N supply.

Root morphologies of ZD958 and DH605 were assessed in 2019. The root biomass of ZD958 increased by 40% after being supplied with mixed N, while that of DH605 did not differ between N forms (Figure S1A). Our analysis of root architecture showed that the root area of ZD958 increased by 22% after being supplied with mixed N, and the root angle did not change significantly (Figure S1B,C). In contrast, the root biomass and root structure of DH605 did not change significantly after being supplied with mixed N (Figure S1).

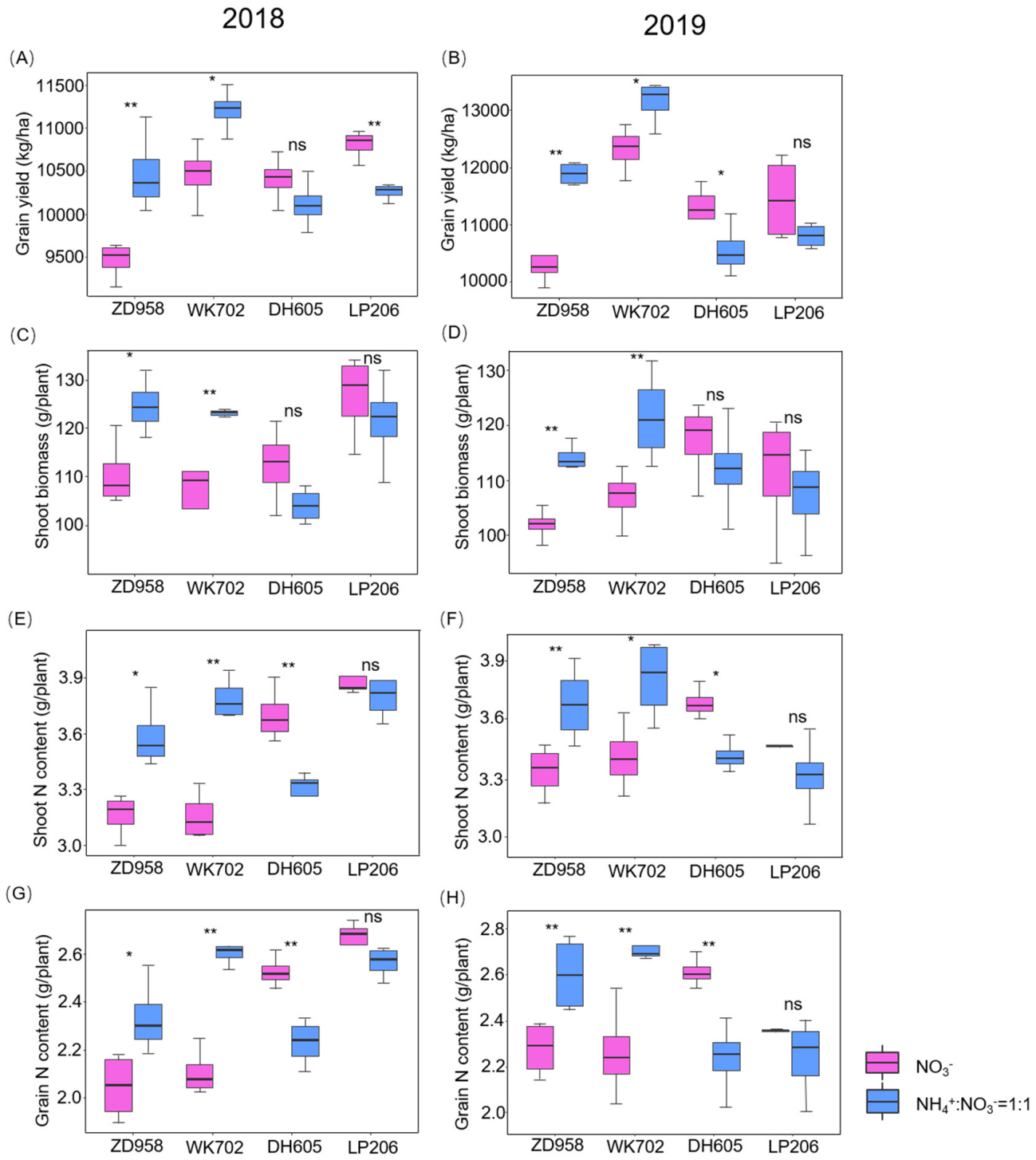

Figure 1. Boxplots for maize grain yield (**A**,**B**), shoot biomass (**C**,**D**), shoot N content (**E**,**F**), and grain N content (**G**,**H**) for ZD958, WK702, DH605 and LP206 in response to nitrate and mixed N supply in 2018 and 2019. The horizontal bars within boxes represent medians. The tops and bottoms of boxes represent the 75th and 25th percentiles, respectively. The whiskers indicate the range of the data. One-way ANOVA followed by an LSD test was performed using R software (3.6.2). ns: not significant ($p > 0.05$). * Significant at $p < 0.05$. ** Significant at $p < 0.01$.

3.2. Diversity and Composition of Root Bacteria and Fungi in Response to N Form and Maize Cultivar

To understand the contribution of cultivar × N form interactions to the diversity and composition of the root microbiome and their effects on the NUE of maize, we selected ZD958 and DH605 for this study due to their differing responses to the N forms. High-throughput sequencing was performed on the rhizospheric and endophytic microbes of these cultivars under two N-form treatments. The rhizospheric microbiome diversities of ZD958 and DH605 differed significantly between the two N-form treatments (Figure S2). ZD958 exhibited higher rhizospheric bacterial diversity compared to DH605 for both N forms, suggesting that ZD958 roots recruited more bacterial species (Figure S2A). Conversely, DH605 had higher rhizosphere fungal diversity than ZD958 for both N forms. Notably, the mixed N supply significantly increased the rhizospheric fungal diversity of ZD958 (Figure S2C). For DH605, the mixed N treatment increased the diversity of rhizospheric bacteria but decreased that of rhizospheric fungi (Figure S2B).

Under a mixed N supply, the Shannon index of DH605 endophytic bacteria was significantly higher than when only nitrate was supplied, whereas ZD958 showed no significant difference between the two N-form treatments (Figure S2B). The endophytic fungal diversity of both ZD958 and DH605 was not affected by the N form, indicating that endophyte diversity was primarily affected by cultivar (Figure S2D). A principal coordinate analysis (PCoA) of Bray–Curtis distances (beta diversity) revealed a distinct rhizospheric bacterial community in DH605 when nitrate or mixed N was supplied (Figure 2A). For ZD958, the rhizospheric fungal community differed significantly between nitrate and mixed N, but this effect was confined to rhizopheric fungi. The community structures of endophytic bacteria and fungi in both maize cultivars showed no significant separation between N-form treatments (Figure 2B–D).

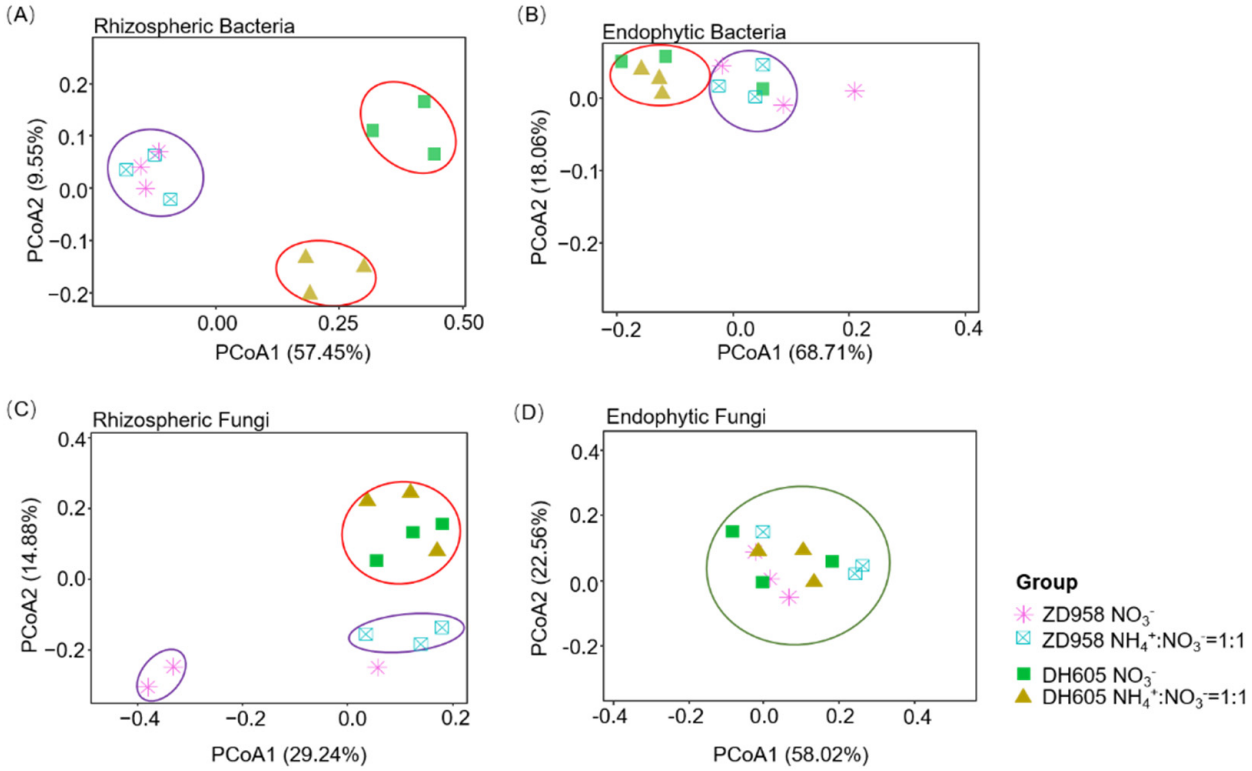

Figure 2. Principal coordinate analysis (PCoA) of (**A**) rhizosphere bacterial community, (**B**) endophytic bacterial community, (**C**) rhizosphere fungal community, and (**D**) endophytic fungal community based on Bray–Curtis distances (beta diversity) for ZD958 and DH605 under nitrate and mixed N supply. $p < 0.001$, permutational multivariate analysis of variance (PERMANOVA) by Adonis.

Figure 3 presents bar graphs showing the changes in the ten most-abundant bacterial phyla and all eight fungal phyla in ZD958 and DH605 under two N-form treatments. Among the rhizospheric bacterial phyla, Proteobacteria, Bacteroidetes, Acidobacteria, and Actinobacteria were the most prevalent, accounting for 28.6–50.3%, 6.4–36.4%, 4.3–14.6%, and 2.6–13.0%, respectively. Proteobacteria and Cyanobacteria were the dominant endophytic bacterial phyla, comprising 96.0–98.2% of the total abundance (Figure 3A). The most abundant fungal phylum across all samples was Basidiomycota, followed by Mortierellomycota, with relative abundances of 68.4–83.1% and 7.1–18.5%, respectively (Figure 3B).

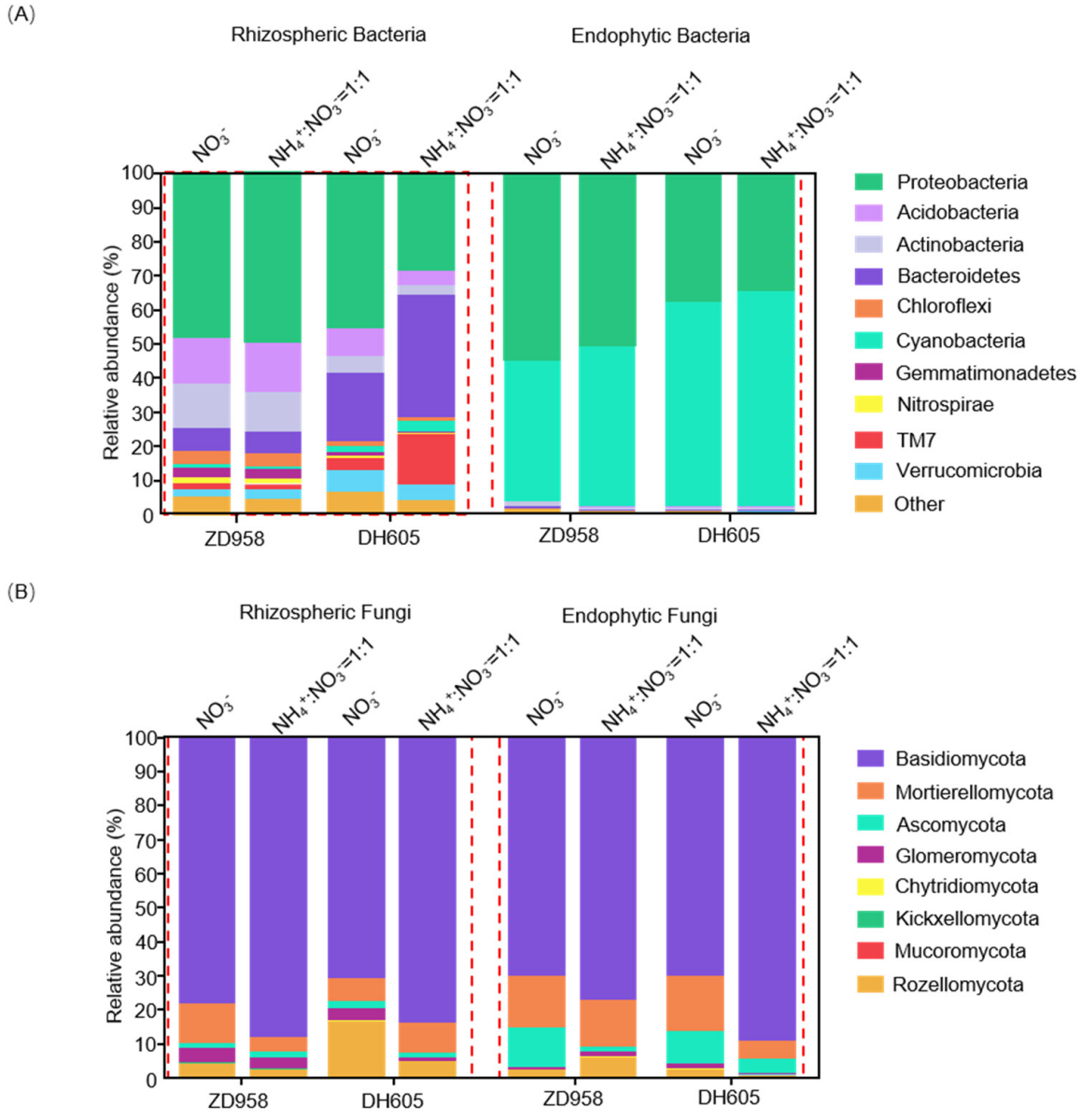

Figure 3. Bar graph depicting the community composition of bacteria (**A**) and fungi (**B**) at the phylum level for ZD958 and DH605 under nitrate and mixed N supply. Different bacteria and fungi phyla are color-coded, with only top-ten bacteria phyla by abundance individually labeled due to space constraints.

For dominant rhizospheric bacterial phyla, the mixed N treatment significantly decreased the relative abundance of Actinobacteria in ZD958 and Proteobacteria and Acidobacteria in DH605 compared to nitrate-N treatment (Figure 4A,B). Conversely, the mixed N treatment significantly increased the relative abundance of Bacteroidetes in DH605 (Figure 4B). Among rhizospheric fungal phyla, the mixed N treatment significantly increased the relative abundance of Basidiomycota in both maize cultivars while decreasing Mortierellomycota and Glomeromycota in DH605 (Figure 4E,F). The relative abundances of endophytic bacterial and fungal phyla did not differ significantly between nitrate-N and mixed N treatments in either ZD958 or DH605 (Figure 4C,D,G,H).

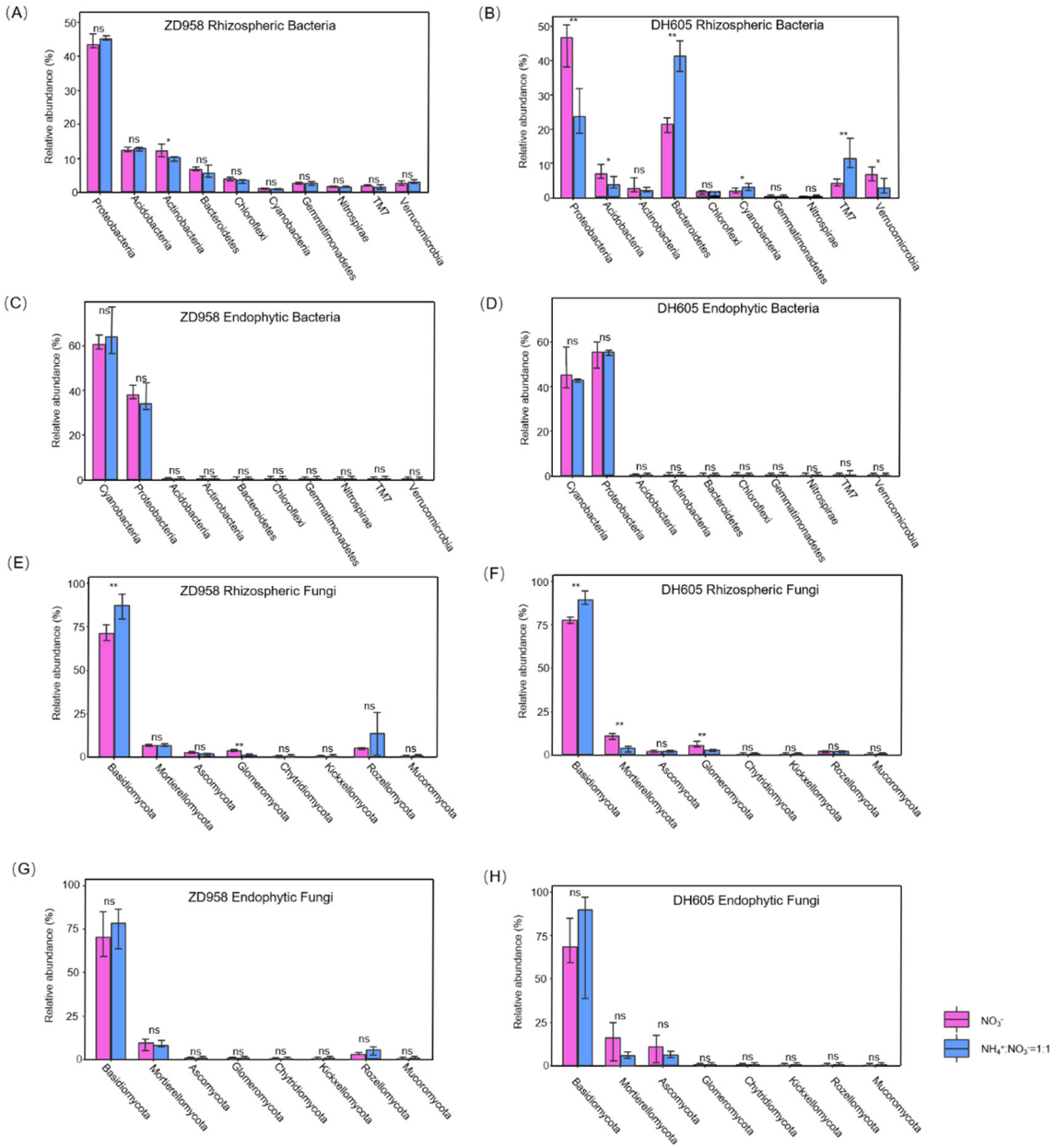

Figure 4. Top-ten changes in rhizospheric bacteria phyla for ZD958 (**A**) and DH605 (**B**), and top-ten changes in endophytic bacteria phyla for ZD958 (**C**) and DH605 (**D**), as well as in all dominant rhizospheric fungal phyla for ZD958 (**E**) and DH605 (**F**), and changes in all dominant endophytic fungal phyla changes for ZD958 (**G**) and DH605 (**H**) in response to nitrate and mixed N supply. One-way ANOVA followed by an LSD test was performed using R software. ns: not significant ($p > 0.05$). * Significant at $p < 0.05$. ** Significant at $p < 0.01$.

These results indicate that root endophytic microorganisms were mainly influenced by the host maize cultivar, while the rhizospheric microorganisms were affected by the interaction of the cultivar and N form. The response of rhizosphere microbe communities differed between ZD958 and DH605: the N form primarily affected the fungi community structure in ZD958 and the bacterial community structure in DH605.

3.3. Difference in Microbial and Biochemical Functions between ZD958 and DH605 Treated with Different N Forms

Many of the OTUs in rhizospheric samples exhibited functions related to the N cycle, which primarily involves bacteria. Using FAPROTAX, a database for converting microbial community profiles into putative functional profiles based on the literature about cultivated strains, we annotated the function of the OTUs in ZD958 and DH605 treated with the two N forms. The rhizospheric OTUs of both cultivars were associated with N pathways, including nitrate synthesis, denitrification, reduction, nitrification, and nitrite synthesis, reflecting the complexity of the N cycle under different N forms (Figure 5). It is noteworthy that under a mixed nitrogen supply, the rhizosphere microorganisms of DH605 exhibit stronger nitrification function than those of ZD958, indicating that maize varieties insensitive to ammonium have a stronger microbial nitrification function, thereby weakening the enhancing effect of ammonium (Figure 5B).

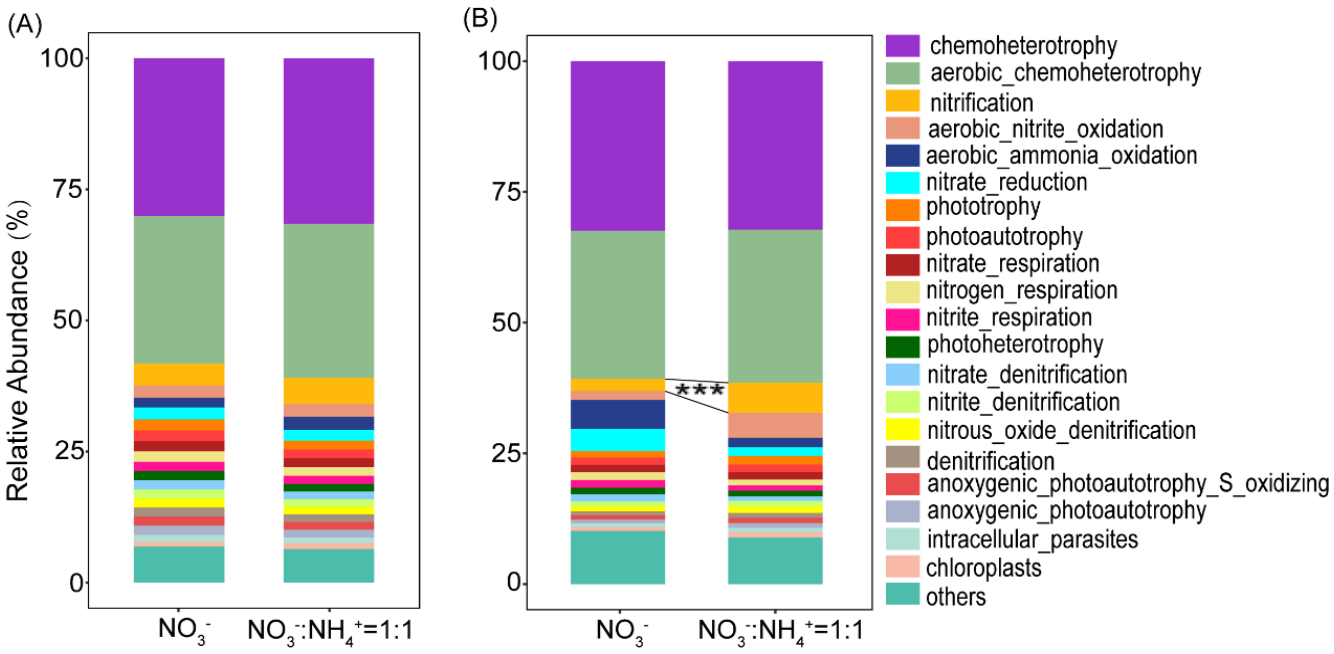

Figure 5. Metabolic and ecological functions prediction for bacterial OTUs in the rhizosphere of ZD958 (**A**) and DH605 (**B**) under nitrate and mixed N supply based on FAPROTAX. One-way ANOVA followed by an LSD test was performed using R software. *** Significant at $p < 0.001$.

3.4. Effects of Root Metabolites on Rhizospheric Bacteria and Fungi

To investigate the influence of host cultivars on the response of rhizosphere microbiota to different N forms, we examined the root metabolome using GC-MS. A total of 373 metabolites were identified, with 14 and 13 differential metabolites (p with FDR-adjusted <0.05, fold-change ≥ 2) identified in ZD958 and DH605 between nitrate and mixed N treatments, respectively (Figures S4 and S5). In ZD958, the mixed N supply significantly increased levels of palmitoleic acid, while other metabolites showed the opposite trend (Figure S5A). In DH605, the mixed N supply significantly increased the levels of isoacteoside, 2-hydroxystearic acid, seaminol.glucoside, L-carnitine, L-acetylcarnitine, tiotropium, propionylcarnitine, gadoteridol, and beta-guanidinopropionic acid, and significantly decreased levels of 5-aminopentanoic acid, 16,17-dihydro-16a,17-dihydroxygibberellin A7

17-glucoside, physangulide and sphinganine (Figure S5B). To further explore the microbiota–metabolite interactions, we evaluated the correlations between dominant rhizospheric bacteria-fungi and differential metabolites (Figure S6). A co-occurrence network graph was constructed to highlight the main in microbiota–metabolite interplays (Spearman's correlation analysis, r > 0.4, $p < 0.05$) (Figure 6).

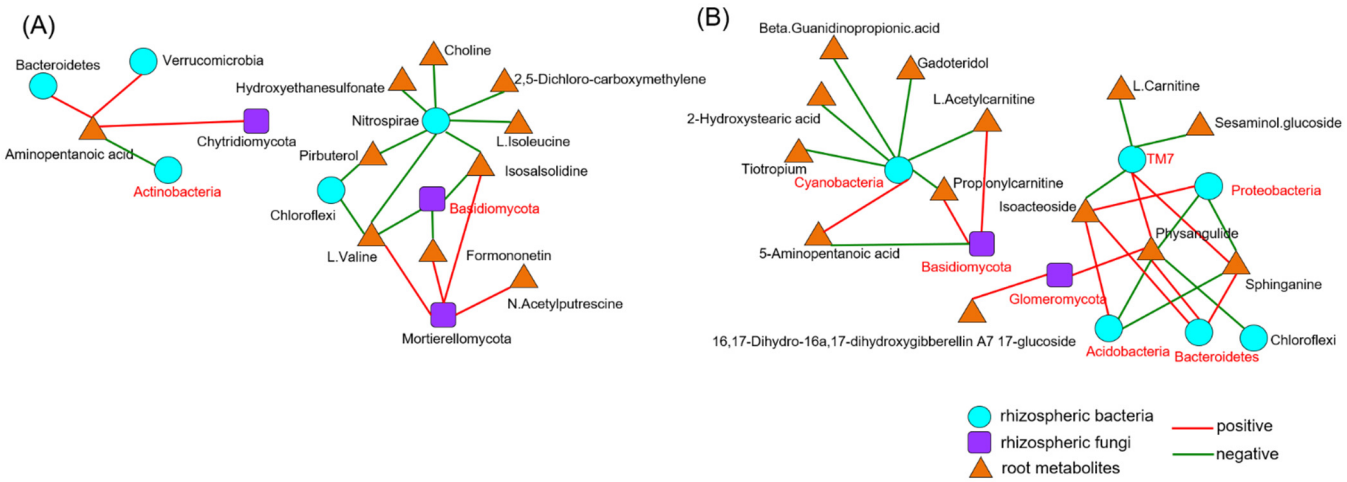

Figure 6. Co-occurrence network of the microbe–metabolite interactions discovered in ZD958 (**A**) and DH605 (**B**) (Spearman's correlation analysis, r > 0.4, $p < 0.05$). Rhizospheric bacteria, rhizospheric fungi, and root metabolites were labeled with turquoise circles, purple squares, and orange triangles, respectively. Red connecting lines represent positive correlations between two nodes, while green connecting lines represent negative correlations. Microbes in red text indicate significant differences in abundance between the two N-form treatments.

In ZD958, Nitrospirae appeared to be the core bacteria phylum, negatively correlated with seven differential metabolites, though it changed a little after the mixed N supply. In addition, the dominant rhizosphere fungus Basidiomycota, which significantly increased in abundance after the mixed N supply, was negatively correlated with isosalsolidine, formononetin and L-Valine. Aminopentanoic acid and L-Valine played key roles in connecting the network. In DH605, Cyanobacteria was the core genus, negatively correlated with six differential metabolites and positively correlated with 5-aminopentanoic acid. Proteobacteria, Acidobacteria, Bacteroidetes and TM7, the dominant phyla in response to mixed N supply, were significantly correlated with isoacteoside, sphinganine and physangulide, acting as key connections within the network.

4. Discussion

Plants acquire N from the soil mainly in the form of nitrate and ammonium. Supplying plants with a mixture of these forms can enhance growth [13], as plants show complex physiological and morphological responses to different N sources [33]. Our two-year field experiments demonstrated that maize cultivars exhibit distinct growth responses to nitrate and mixed N supplies, extending to the root microbiome (Figure 1). Compared with nitrate N, mixed nitrate and ammonium significantly increased the grain yield and N contents of ZD958 and WK702, which are sensitive to ammonium. However, the growth-promoting effect of ammonium was not observed in LP206 and DH605, which are classified as ammonium-insensitive cultivars (Table S1). This difference in response to NH_4^+-N was consistent across years, indicating the cultivar-specific control of growth responses to N forms [34]. Therefore, using NH_4^+-N-sensitive maize cultivars and the rational application of N fertilizer could boost maize production and NUE without extra N input [35,36]. Further research is needed to understand the genetic and molecular mechanisms underlying crop responses to different N forms [37].

Root microbiomes indicate that rhizospheric microbial communities are largely influenced by soil type, while root endophytes are primarily determined by plant species [38]. Our study confirmed that rhizospheric bacterial and fungal communities were affected by both the N form and maize cultivars, whereas endophytic microbial communities were mainly influenced by maize cultivars (Figures 2 and S2). Genotype × environment interactions determine the composition of the root microbiome [39,40]. Here, rhizospheric bacteria and fungi showed cultivar × N form responses. The mixed N treatment significantly affected the rhizosphere fungal community in ZD958 and the bacterial community in DH605 (Figure 2). For ZD958, the mixed N treatment significantly increased the relative abundance of Basidiomycota in the rhizospheric fungi (Figure 4), and there was a significant positive correlation ($p = 0.02$) between the relative abundance of Basidiomycota and grain yield in ZD958 (Figure S3). This suggests that the increase in Basidomycota abundance in the rhizospheric fungi was crucial for promoting ZD958 growth with mixed N supply. Additionally, ZD958 had higher root biomasses and larger root areas with mixed N (Figure S1A,B), potentially enhancing mycorrhizal fungi colonization and nutrient uptake [41].

N-form transformation is primarily carried out by bacteria, not fungi [14]. For DH605, the mixed N supply changed the relative abundance of Bacteroidetes and Proteobacteria in the rhizospheric bacteria (Figure 4B), which participated in N transformation [14]. Functional predictions indicated stronger nitrification in DH605 after the mixed N treatment (Figure 5), which may explain the lack of significant phenotype changes under ammonium-enhanced conditions. Further validation of these bacterial functions is needed. Fungi and bacteria may mutually stabilize the rhizosphere under different N-form treatments [42].

Significant differences in rhizospheric microbial community compositions among maize cultivars treated with different N forms were observed (Figures 4 and 5). Root metabolites and exudates likely drive these changes [43]. Root-secreted secondary metabolites can attract growth-promoting rhizobacteria and arbuscular mycorrhizal (AM) fungi, which are essential for plant growth and defense [44,45]. In this study, palmitoleic acid levels were significantly higher in ZD958 roots treated with mixed N than with nitrate (Figure S4). Palmitoleic acid, an organic acid secreted by root exudates, recruits growth-promoting rhizobacteria and AM fungi [46,47]. Therefore, ZD958 roots could recruit more beneficial rhizospheric fungi to enhance plant growth and N uptake by synthesizing and secreting more palmitoleic acid when supplied with mixed N.

Previous research has shown a close relationship between the root microbiome and root metabolites [48–50]. We found that changes in maize-root metabolism under different N forms were closely related to specific rhizospheric bacterial and fungal phyla (Figures 6 and S5). In DH605, sphinganines were significantly negatively correlated with Acidobacteria and Proteobacteria and positively correlated with Bacteroidetes and TM7 (Figure 6B). Sphinganine is involved in cell adhesion, migration, and invasion, crucial for microbe–metabolite interaction [51]. In DH605, the mixed N supply significantly decreased root sphinganine metabolism compared to only nitrate supply (Figure S4), possibly explain the strong bacterial community response to mixed N. The co-occurrence network revealed stronger correlations between rhizospheric bacteria and fungi in DH605 than in ZD958 (Figure 6), suggesting that NH_4^+-N-sensitive maize cultivars have more root metabolites involved in ammonium absorption and assimilation than microbial recruitment under a mixed N supply. In the future, we need to utilize molecular biology techniques to conduct more sophisticated research on corn genes and microorganisms, and the current research has laid a solid foundation for this work.

5. Conclusions

Our results showed that maize cultivars differ in their response to N forms, particularly in biomass growth and N uptake. These differences drive changes in the root microbiome through cultivar and N-form interactions. N forms mainly affect rhizospheric bacteria microbes, not endophytic microbes. Specifically, mixed N increased the relative abundance of Basidiomycota in ZD958, positively correlated with its grain yield, while DH605 exhibited

a stronger nitrification function, weakening the ammonium N effect. We also found that root metabolites differed between the two N forms and were closely related to specific rhizospheric bacteria and fungi communities. Taken together, our results enhance the understanding of the relationships between maize cultivars and their associated microbial communities in response to N forms, with significant implications for improving nutrient efficiency in plant–soil systems. In the future, we need to use molecular biology methods to reveal more detailed theoretical mechanisms in a more perfect way.

Supplementary Materials: The following supporting information can be downloaded at: https://www.mdpi.com/article/10.3390/agronomy14081828/s1.

Author Contributions: G.T.: Investigation, Methodology, Software, Data curation, Formal analysis, Writing—original draft. W.R. and J.X.: Formal analysis, Methodology, Writing—review and editing. X.L.: Data curation, Methodology, Formal analysis. J.L.: Writing—review and editing. G.M.: Conceptualization, Writing—review and editing. X.G. and F.C.: Conceptualization, Methodology, Software, Data curation, Formal analysis, Writing—review and editing, Supervision. All authors have read and agreed to the published version of the manuscript.

Funding: This work is supported by the National Key Research and Development Program of China (2021YFD1900600), the National Science Foundation of China (31972485, 32202587) and the Inner Mongolia Autonomous Region Science and Technology Plan (2022YFHH0021).

Data Availability Statement: The raw sequence data reported in this paper have been deposited at NCBI and are available for public inspection at PRJNA930688.

Acknowledgments: The anonymous reviewers have also contributed considerably to the publication of this paper.

Conflicts of Interest: The researcher claims there are no conflicts of interests.

References

1. Müller, C.A.; Obermeier, M.M.; Berg, G. Bioprospecting plant-associated microbiomes. *J. Biotechnol.* **2016**, *235*, 171–180. [CrossRef] [PubMed]
2. Berendsen, R.; Pieterse, C.M.J.; Bakker, P.A.H.M. The rhizosphere microbiome and plant health. *Trends Plant Sci.* **2012**, *17*, 478–486. [CrossRef] [PubMed]
3. Bai, B.; Liu, W.D.; Qiu, X.Y.; Zhang, J.; Zhang, J.Y.; Bai, Y. The root microbiome: Community assembly and its contributions to plant fitness. *J. Integr. Plant Biol.* **2022**, *64*, 230–243. [CrossRef]
4. Tilman, D.; Balzer, C.; Hill, J.; Befort, B.L. Global food demand and the sustainable intensification of agriculture. *Proc. Natl. Acad. Sci. USA* **2011**, *108*, 20260–20264. [CrossRef] [PubMed]
5. Raun, W.R.; Johnson, G.V. Improving Nitrogen Use Efficiency for Cereal Production. *Agron. J.* **1999**, *91*, 357–363. [CrossRef]
6. Li, S.; Zhang, H.; Wang, S.; Shi, L.; Xu, F.; Wang, C.; Cai, H.; Ding, G. The rapeseed genotypes with contrasting NUE response discrepantly to varied provision of ammonium and nitrate by regulating photosynthesis, root morphology, nutritional status, and oxidative stress response. *Plant Physiol. Biochem.* **2021**, *166*, 348–360. [CrossRef] [PubMed]
7. Miller, A.; Cramer, M. Root nitrogen acquisition and assimilation. *Plant Soil* **2005**, *274*, 1–36. [CrossRef]
8. González-Prieto, S.J.; Beaupied, H.; Moiroud, A.; Domenach, A.M. Uniformity of labelling of alder leaves fertilized with NH_4^+-15N and NO_3^--15N by roots or leaves. *Soil Biol. Biochem.* **1995**, *27*, 1559–1563. [CrossRef]
9. Li, S.X.; Wang, Z.H.; Stewart, B.A. Responses of Crop Plants to Ammonium and Nitrate N. *Adv. Agron.* **2013**, *118*, 205–397. [CrossRef]
10. Naz, S.; Shen, Q.; Lwalaba, J.L.W.; Zhang, G. Genotypic Difference in the Responses to Nitrogen Fertilizer Form in Tibetan Wild and Cultivated Barley. *Plants* **2021**, *10*, 595. [CrossRef]
11. Swailam, M.A.; Mowafy, S.A.E.; El-Naggar, N.Z.A.; Mansour, E. Agronomic responses of diverse bread wheat genotypes to phosphorus levels and nitrogen forms in a semiarid environment. *J. Breed. Genet.* **2021**, *53*, 592–608. [CrossRef]
12. George, J.; Holtham, L.; Sabermanesh, K.; Heuer, S.; Tester, M.; Plett, D.; Garnett, T. Small amounts of ammonium (NH_4^+) can increase growth of maize (*Zea mays*). *J. Plant Nutr. Soil Sci.* **2016**, *179*, 717–725. [CrossRef]
13. Wang, P.; Wang, Z.; Pan, Q.; Sun, X.; Chen, H.; Chen, F.; Yuan, L.; Mi, G. Increased biomass accumulation in maize grown in mixed nitrogen supply is mediated by auxin synthesis. *J. Exp. Bot.* **2019**, *70*, 1859–1873. [CrossRef] [PubMed]
14. Kuypers, M.M.M.; Marchant, H.K.; Kartal, B. The microbial nitrogen-cycling network. *Nat. Rev. Microbiol.* **2018**, *16*, 263–276. [CrossRef] [PubMed]
15. Zhu, G.; Wang, X.; Wang, S.; Yu, L.; Armanbek, G.; Yu, J.; Jiang, L.; Yuan, D.; Guo, Z.; Zhang, H.; et al. Towards a more labor-saving way in microbial ammonium oxidation: A review on complete ammonia oxidization (comammox). *Sci. Total Environ.* **2022**, *829*, 154590. [CrossRef] [PubMed]

16. Pachiadaki, M.G.; Sintes, E.; Bergauer, K.; Brown, J.M.; Record, N.R.; Swan, B.K.; Mathyer, M.E.; Hallam, S.J.; Lopez-Garcia, P.; Takaki, Y.; et al. Major role of nitrite-oxidizing bacteria in dark ocean carbon fixation. *Science* **2017**, *358*, 1046–1051. [CrossRef] [PubMed]
17. Ketsa, S.; Atantee, S. Nitrification in soil -Terminology and methodology (review). *Rostl. Vyrob.* **2000**, *46*, 385–395. [CrossRef]
18. Yu, C.; Hu, X.M.; Deng, W.; Li, Y.; Xiong, C.; Ye, H.; Han, G.M.; Li, X. Changes in soil microbial community structure and functional diversity in the rhizosphere surrounding mulberry subjected to long-term fertilization. *Appl. Soil Ecol.* **2015**, *86*, 30–40. [CrossRef]
19. Liu, Y.M.; Cao, W.Q.; Chen, X.X.; Yu, B.G.; Lang, M.; Chen, X.P.; Zou, C.Q. The responses of soil enzyme activities, microbial biomass and microbial community structure to nine years of varied zinc application rates. *Sci. Total Environ.* **2020**, *737*, 140245. [CrossRef]
20. Bruez, E.; Vallance, J.; Gerbore, J.; Lecomte, P.; Costa, J.P.D.; Guerin-Dubrana, L.; Rey, P. Analyses of the Temporal Dynamics of Fungal Communities Colonizing the Healthy Wood Tissues of Esca Leaf-Symptomatic and Asymptomatic Vines. *PLoS ONE* **2014**, *9*, e95928. [CrossRef]
21. Schlatter, D.C.; Bakker, M.G.; Bradeen, J.M.; Kinkel, L.L. Plant community richness and microbial interactions structure bacterial communities in soil. *Ecology* **2016**, *96*, 134–142. [CrossRef] [PubMed]
22. Li, Q.; Song, X.; Gu, H.; Gao, F. Nitrogen deposition and management practices increase soil microbial biomass carbon but decrease diversity in Moso bamboo plantations. *Sci. Rep.* **2016**, *6*, 28235. [CrossRef]
23. Zhou, Z.F.; Shi, X.J.; Zheng, Y.; Qin, Z.X.; Xie, D.T.; Li, Z.L.; Guo, T. Abundance and community structure of ammonia-oxidizing bacteria and archaea in purple soil under long-term fertilization. *Eur. J. Soil Biol.* **2014**, *60*, 24–33. [CrossRef]
24. Chen, Y.L.; Xu, Z.W.; Hu, H.W.; Hu, Y.J.; Hao, Z.P.; Jiang, Y.; Chen, B.D. Responses of ammonia-oxidizing bacteria and archaea to nitrogen fertilization and precipitation increment in a typical temperate steppe in Inner Mongolia. *Appl. Soil Ecol.* **2013**, *68*, 36–45. [CrossRef]
25. Zou, W.; Lang, M.; Zhang, L.; Liu, B.; Chen, X.P. Ammonia-oxidizing bacteria rather than ammonia-oxidizing archaea dominate nitrification in a nitrogen-fertilized calcareous soil. *Sci. Total Environ.* **2022**, *811*, 151402. [CrossRef] [PubMed]
26. Ibrahim, M.M.; Tong, C.; Hu, K.; Zhou, B.; Xing, S.; Mao, Y. Biochar-fertilizer interaction modifies N-sorption, enzyme activities and microbial functional abundance regulating nitrogen retention in rhizosphere soil. *Sci. Total Environ.* **2020**, *739*, 140065. [CrossRef]
27. Dai, Z.M.; Su, W.Q.; Chen, H.H.; Barberán, A.; Zhao, H.C.; Yu, M.J.; Yu, L.; Brookes, P.C.; Schadt, C.W.; Chang, S.X.; et al. Long-term nitrogen fertilization decreases bacterial diversity and favors the growth of Actinobacteria and Proteobacteria in agro-ecosystems across the globe. *Glob. Chang. Biol.* **2018**, *24*, 3452–3461. [CrossRef] [PubMed]
28. Koprivova, A.; Schwier, M.; Volz, V.; Kopriva, S. Shoot-root interaction in control of camalexin exudation in *Arabidopsis*. *J. Exp. Bot.* **2023**, *18*, erad031. [CrossRef]
29. Mahmood, T.; Woitke, M.; Gimmler, H.; Kaiser, W.M. Sugar exudation by roots of kallar grass [*Leptochloa fusca* (L.) Kunth] is strongly affected by the nitrogen source. *Planta* **2002**, *214*, 887–894. [CrossRef]
30. Ravazzolo, L.; Trevisan, S.; Manoli, A.; Boutet-Mercey, S.P.; Perreau, F.O.; Quaggiotti, S. The Control of Zealactone Biosynthesis and Exudation is Involved in the Response to Nitrogen in Maize Root. *Plant Cell Physiol.* **2019**, *60*, 2100–2112. [CrossRef]
31. Liu, Z.; Zhao, Y.; Guo, S.; Cheng, S.; Guan, Y.; Cai, H.; Mi, G.; Yuan, L.; Chen, F. Enhanced crown root number and length confers potential for yield improvement and fertilizer reduction in nitrogen-efficient maize cultivars. *Field Crop. Res.* **2019**, *241*, 107562. [CrossRef]
32. Shao, H.; Shi, D.F.; Shi, W.J.; Ban, X.B.; Chen, Y.C.; Ren, W.; Chen, F.J.; Mi, G.H. Genotypic difference in the plasticity of root system architecture of field-grown maize in response to plant density. *Plant Soil* **2019**, *439*, 201–217. [CrossRef]
33. Hachiya, T.; Sakakibara, H. Interactions between nitrate and ammonium in their uptake, allocation, assimilation, and signaling in plants. *J. Exp. Bot.* **2017**, *68*, 2501–2512. [CrossRef] [PubMed]
34. Al-Naggar, A.M.M.; Shabana, R.A.; Atta, M.M.M.; Al-Khalil, T.H. Maize response to elevated plant density combined with lowered N-fertilizer rate is genotype-dependent. *Crop J.* **2015**, *3*, 96–109. [CrossRef]
35. Bloom, A.J.; Sukrapanna, S.S.; Warner, R.L. Root Respiration Associated with Ammonium and Nitrate Absorption and Assimilation by Barley. *Plant Physiol.* **1992**, *99*, 1294–1301. [CrossRef]
36. Cramer, M.D.; Lewis, O.A.M. The Influence of Nitrate and Ammonium Nutrition on the Growth of Wheat (*Triticum aestivum*) and Maize (*Zea mays*) Plants. *Ann. Bot.* **1993**, *72*, 359–365. [CrossRef]
37. Ke, F.; Wang, X.L. Nitrate Uptake of Rice as Affected by Growth Stages and Ammonium. *Agric. Sci. China* **2003**, *002*, 62–67.
38. Xiao, X.; Chen, W.; Zong, L.; Yang, J.; Jiao, S.; Lin, Y.; Wang, E.; Wei, G. Two cultivated legume plants reveal the enrichment process of microbiome in the rhizocompartments. *Mol. Ecol.* **2017**, *26*, 1641–1651. [CrossRef]
39. Gallart, M.; Adair, K.L.; Love, J.; Meason, D.F.; Clinton, P.W.; Xue, J.; Turnbull, M.H. Host Genotype and Nitrogen Form Shape the Root Microbiome of *Pinus radiata*. *Microb. Ecol.* **2018**, *75*, 419–433. [CrossRef]
40. Giagnoni, L.; Pastorelli, R.; Mocali, S.; Arenella, M.; Nannipieri, P.; Renella, G. Availability of different nitrogen forms changes the microbial communities and enzyme activities in the rhizosphere of maize lines with different nitrogen use efficiency. *Appl. Soil Ecol.* **2016**, *98*, 30–38. [CrossRef]
41. Tarkka, M.T.; Drigo, B.; Deveau, A. Mycorrhizal microbiomes. *Mycorrhiza* **2018**, *28*, 403–409. [CrossRef]

42. Chen, S.M.; Waghmode, T.R.; Sun, R.B.; Kuramae, E.E.; Hu, C.S.; Liu, B.B. Root-associated microbiomes of wheat under the combined effect of plant development and nitrogen fertilization. *Microbiome* **2019**, *7*, 136. [CrossRef] [PubMed]
43. Zhalnina, K.; Louie, K.B.; Hao, Z.; Mansoori, N.; Rocha, U.N.; Shi, S.; Cho, H.; Karaoz, U.; Loqué, D.; Bowen, B.P.; et al. Dynamic root exudate chemistry and microbial substrate preferences drive patterns in rhizosphere microbial community assembly. *Nat. Microbiol.* **2018**, *3*, 470–480. [CrossRef]
44. Walker, T.S.; Bais, H.P.; Grotewold, E.; Vivanco, J.M. Root Exudation and Rhizosphere Biology. *Plant Physiol.* **2003**, *132*, 44–51. [CrossRef] [PubMed]
45. Rolfe, S.A.; Griffiths, J.; Ton, J. Crying out for help with root exudates: Adaptive mechanisms by which stressed plants assemble health-promoting soil microbiomes. *Curr. Opin. Microbiol.* **2019**, *49*, 73–82. [CrossRef]
46. Kameoka, H.; Tsutsui, I.; Saito, K.; Kikuchi, Y.; Handa, Y.; Ezawa, T.; Hayashi, H.; Kawaguchi, M.; Akiyama, K. Stimulation of asymbiotic sporulation in arbuscular mycorrhizal fungi by fatty acids. *Nat. Microbiol.* **2019**, *4*, 1654–1660. [CrossRef] [PubMed]
47. Xiong, Y.W.; Li, X.W.; Wang, T.T.; Gong, Y.; Zhang, C.M.; Xing, K.; Qin, S. Root exudates-driven rhizosphere recruitment of the plant growth-promoting rhizobacterium Bacillus flexus KLBMP 4941 and its growth-promoting effect on the coastal halophyte *Limonium sinense* under salt stress. *Ecotoxicol. Environ. Saf.* **2020**, *194*, 110374. [CrossRef] [PubMed]
48. Bendaly, A.; Messedi, D.; Smaoui, A.; Ksouri, R.; Bouchereau, A.; Abdelly, C. Physiological and leaf metabolome changes in the xerohalophyte species *Atriplex halimus* induced by salinity. *Plant Physiol. Biochem.* **2016**, *103*, 208–218. [CrossRef]
49. Wang, W.; Yang, X.; Tangchaiburana, S.; Ndeh, R.; Markham, J.E.; Tsegaye, Y.; Dunn, T.M.; Wang, G.L.; Bellizzi, M.; Parsons, J.F.; et al. An inositolphosphorylceramide synthase is involved in regulation of plant programmed cell death associated with defense in *Arabidopsis*. *Plant Cell* **2008**, *20*, 3163–3179. [CrossRef]
50. Greenberg, J.T.; Silverman, F.P.; Liang, H. Uncoupling salicylic acid-dependent cell death and defense-related responses from disease resistance in the Arabidopsis mutant acd5. *Genetics* **2000**, *156*, 341–350. [CrossRef] [PubMed]
51. Michaelson, L.V.; Zäuner, S.; Markham, J.E.; Haslam, R.P.; Desikan, R.; Mugford, S.; Albrecht, S.; Warnecke, D.; Sperling, P.; Heinz, E.; et al. Functional characterization of a higher plant sphingolipid Delta4-desaturase: Defining the role of sphingosine and sphingosine-1-phosphate in Arabidopsis. *Plant Physiol.* **2009**, *149*, 487–498. [CrossRef]